Robust Target Localization for Multistatic Passive Radar Networks

Linjie Yan[1], Luca Pallotta[2*], Gaetano Giunta[3*], and Danilo Orlando[4*],

[1] Institute of Acoustics, Chinese Academy of Sciences, 100190 Beijing, China
[2] School of Engineering, University of Basilicata, 85100 Potenza, Italy
[3] Industrial, Electronic and Mechanical Engineering Department, University of Roma Tre, 00146 Rome, Italy
[4] Università degli Studi "Niccolò Cusano", 00166 Roma, Italy
[*] Senior Member, IEEE

Abstract—Passive multistatic radar networks localize a non-cooperative target exploiting the bistatic measurements associated with signals emitted by several transmitters of opportunity and acquired by multiple receivers. However, in realistic scenarios, it might happen that one or more receivers are damaged and/or under malicious attacks with a consequent degradation of the system performance. This paper proposes a procedure to reveal sensors that return anomalous measurements due to an attack or a failure. Specifically, we first detect such measurements by solving a binary hypothesis test, then we cancel them and estimate the final delays as well as the target position. The performance of the overall architecture is assessed using both synthetic data and real-recorded data.

Index Terms—Cross-cross-correlation, failure detection, passive coherent location, passive multistatic radar, transmitter of opportunity.

I. INTRODUCTION

Passive radar systems [1], [2] are widely used to detect, localize, and track non-cooperative targets. In a multistatic radar network [3], these tasks are accomplished by means of two antennas: one antenna points towards the source of opportunity to record the transmitted waveform, whereas the second is used to collect echoes backscattered by the target. At the receiver side, the elliptic localization is commonly performed by exploiting the classic cross-correlation (CC) procedure for each bistatic measurement [4], [5]. In recent years, many algorithms aimed at improving the accuracy in target position estimate with a passive coherent location (PCL) system under the ideal situation in which all receivers correctly work have been developed [4]–[7]. However, in practice, one or more sensors could return erroneous measurements due, for instance, to jamming attacks, unintentional interference, or hardware failures [8]. Thus, the set of measurements used for localization can contain outliers that, if not properly handled, can lead to a severe localization performance degradation. Even though there exist many studies considering the problem of outlier identification within a set of time difference of arrival (TDOA) measurements (see [9]–[11]), in the case of a complete fault of a sensor, the rejection of such outliers could be not sufficient to restore the performance. Similarly, even though during the data association process, erroneous measurements can be eliminated, it is necessary also to identify and discard a sensor whose behavior is anomalous due to an internal failure or, remarkably, to an external attack from a malicious platform. In fact, in above situations, to guarantee a reliable localization performance it would be necessary to perform a prior identification of the faulty sensor and reject all measurements returned by it. In this respect, in [12] an architecture based on the outlier distribution of the TDOA equations has been designed to properly detect the faulty receiver in a passive radar network that uses the signal emitted by the target.

In this paper, we extend the procedure proposed in [12] from hyperbolic to elliptic localization using opportunity signals at different portions of the available spectrum. Hence, the bistatic signal emitted by an independent source and reflected by the target towards the receiver is exploited in the localization process. As a consequence, the reflected signal has a very low signal to noise ratio (SNR). Differently, the model in [12] uses the replicas of the signal directly emitted by the target, that experience a possible higher SNR. For these reasons, we introduce two levels of failure that are handled to make more robust the new fault sensor detection procedure with respect to that proposed in [12]. The main technical contributions of this work can be summarized as:

- all the equation involved in the localization are clustered into three nonoverlapped groups, i.e., strong outliers, weak outliers, and normal, according to their impact on the Least Squares (LS) problem;
- differently from [12], where outlier equations are sequentially removed, in this paper not because of a lower dimension of the related LS problem (in fact, in the PCL, the second-order correlations are computed, at each node, only between the direct opportunity signal and its bistatic counterpart). Then, only after that a receiver is declared in failure, its corresponding equations are removed and the final bistatic delays are estimated;
- the warning score associated to each sensor is weighted on the basis of the cluster to which the returned measurements belong. In this way, the impact of the outlier equations is diversified.

Finally, the detection of a faulty sensor is obtained from a binary hypothesis test accounting for the warning score distribution as in [12] (the warning score distribution differs from that in [12] in terms of weights applied in the warning computation and number of sensors involved in each equation). The illustrative examples are obtained on both synthetic and real-recorded data and show the capability of the proposed procedure in correctly identifying the faulty sensor with consequent accurate bistatic delay estimates.

II. A BRIEF REVIEW OF THE DELAY ESTIMATION PROBLEM

The operating scenario for a passive multistatic radar comprising a non-cooperative target is shown in Fig. 1, where $T \in \mathbb{N}$ transmitters, occupying nonoverlapping frequency bands, and $S \in \mathbb{N}$ receivers

Corresponding author: Linjie Yan (e-mail: yanlinjie16@163.com).

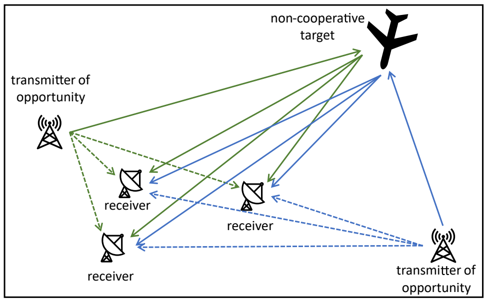

Fig. 1. Graphical illustration of a passive multistatic radar scenario.

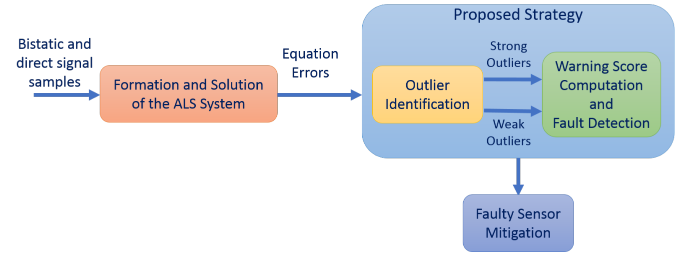

Fig. 2. Block scheme of the proposed algorithm for delays estimation accounting for sensor failure.

are present. Let us denote by $x_{s,t}(nt_s)$, $s = 1, \ldots, S$, $t = 1, \ldots, T$, the bistatic signal received by the sth node and emitted by the tth transmitter, sampled at nt_s with t_s the sampling time. The samples from the reference direct signal recorded by the sth receiving antenna that looks at the tth transmitter of opportunity is indicated by $x_{0,s,t}(nt_s)$, $s = 1, \ldots, S$, $t = 1, \ldots, T$. Applying the classic CC framework, the relative delays $\tau_{0,s,t}$, $s = 1, \ldots, S$, $t = 1, \ldots, T$, between the bistatic and direct signals related to the sth receiver and tth transmitter can be estimated by maximizing the modulus of the discrete-time CC estimate (recall that the signals emitted by the transmitters are separable). As an alternative, the delay estimation problem can be solved also resorting to the cross-cross- and the flipped cross-cross-correlation (CCC) between couples of receivers [13]. The new problem results in an overdetermined system of equations of size $Q = S(S-1)$. The above two methods can be further combined in order to exploit all the possible equations in a more comprehensive system that can be solved using the augmented least squares (ALS) approach.

III. FAILURE DETECTION ALGORITHM

In this section, we describe the proposed method to detect the faulty sensors. To this end, in Figure 2 we show the block-scheme of the entire localization system that comprises the part devoted to the identification of the anomalous sensors. This part is contained in the blue box and consists of a first stage aimed at labeling the equations as possible outliers and a second stage responsible for the computation of the so-called *warning scores* (this concept will be better explained below) and the final detection of the faulty sensor.

Starting from the first stage, the procedure to label the equations of the ALS system as possible outliers is similar to that developed in [12] with the difference that three different labels can be assigned to an equation according to the error deviation, whereas in [12] one outlier level only is considered. Specifically, an outlier is declared each time an entry in the vector containing the absolute errors of each equation in the ALS system exceeds a specific threshold that is set according to the median absolute deviation criterion [14]. The threshold value is a function of a tuning parameter κ aimed at ruling the deepness of outlier identification. Thus, differently from [12], we use such a parameter to cluster all the equation into three not overlapped groups. More precisely, the considered clusters are:

- strong outliers: the equations whose errors overcome the threshold associated with $\kappa = 3$;
- weak outliers: the equations with errors belonging to the interval for which $2 \leq \kappa < 3$;
- normal: all the other cases.

The above choice is motivated by the fact that a high value of κ is overcame by the "wrongest" equations, whereas with $2 \leq \kappa < 3$ all equations that can be still considered erroneous but in a weak sense.

The second stage computes a warning score for each sensor to decide whether or not this sensor is faulty. To this end, it exploits the two levels of outlier returned by the previous stage by assigning a corresponding weight. More in detail, we assign a weight equal to 3 to the equations labeled as strong outliers and a weight equal to 2 in the case of a weak outlier.[1] Then, the warning score for a given sensor is computed by accumulating the weights assigned to the equations involving such a sensor. To this end, when the outlier equation arises from the application of the CC method only the measurement from 1 sensor are used, whereas in the case of the CCC procedure, the equations involve data from 2 sensors. It is evident that in the presence of a faulty sensor, several equations should be marked as outliers with the warning score of the specific sensor being much higher than the others. Conversely, in a normal situation where all sensors are correctly working, the final warning score for each sensor should be low and very close to the others because of the noise impact only. Finally, for each receiver, the binary hypothesis test is applied to declare that the receiver is in failure

$$x^{(i)} \underset{H_{F,0}}{\overset{H_{F,1}}{\gtrless}} \eta_F, \tag{1}$$

where $x^{(i)}$ is the warning score computed for the ith sensor, $H_{F,0}$ is the null hypothesis of normal working, $H_{F,1}$ is the alternative hypothesis of faulty receiver, and η_F is the detection threshold set according to the probability of false failure detection. The pseudo-code of the failure detection procedure is reported in Algorithm 1, where N_p^o, $p = 1, 2$ and $o = s, w$, is the number of strong (s) or weak (w) outlier equations associated with 1 or 2 sensors.

As to the threshold computation, notice that, under $H_{F,0}$, in the case of strong outliers (with weights equal to 3), the warning score is modeled as a binomial random variable with parameters N_p^s and p/TS taking on values $0, 3, 6, \ldots, 3N_p^s$, i.e., $x_p^s \sim \mathcal{B}(N_p^s, p/TS)$. In the same way, in the case of weak outliers (with weights equal to 2), the warning score is modeled as a binomial random variable with parameters N_w^s and p/TS taking on values $0, 2, 4, \ldots, 2N_p^w$, i.e., $x_p^w \sim \mathcal{B}(N_p^w, p/TS)$. The total number of warning scores for a given receiver is obtained by summing the four above-defined warnings, i.e., $x = x_1^s + x_2^s + x_1^w + x_2^w$. Assuming a fully random model for the

[1]Note that, differently from here, in [12], because of the sequential cancellation, all warnings were computed with a weight equal to 1 for all considered outliers.

Algorithm 1 Proposed failure detection algorithm.

Input: Indices of the equations labeled as outliers.
Output: Indices of detected faulty sensors.

1: Count N_1^s, N_2^s, N_1^w, and N_2^w;
2: Compute the warning scores $x^{(i)}$, $i = 1, \ldots, S$;
3: Set the threshold η_F that ensures the desired nominal false failure rate for the parameters N_1^s, N_2^s, N_1^w, and N_2^w;
4: Test $x^{(i)}$, $i = 1, \ldots, S$, through (1).

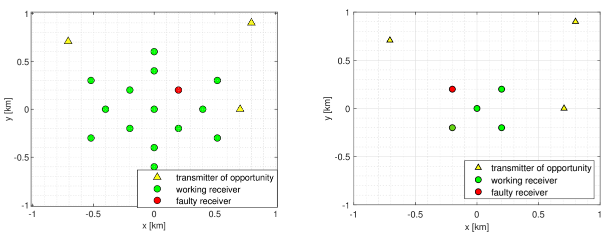

(a) simulated data (b) real-recorded data

Fig. 3. Geometric configuration of the passive multistatic system for (a) simulated data and (b) real-recorded data.

warning scores and also statistical independence between x_1^s, x_2^s, x_1^w, and x_2^w, the probability mass function (pmf) of the random variable x can be computed through the convolution of the pmfs of each component. This pmf can be used to select the detection threshold.

IV. Study Cases

In this section, we prove the effectiveness of the proposed framework, referred to as estimation with failure detection (EFD), in comparison with the positioning algorithm that a priori knows the faulty sensors. It is important to stress that the method devised in [12] for TDOA is not reported in this paper since it completely fails because of the low number of equations in the ALS problem of the multistatic system. Tests are performed by considering the bidimentional (2D) localization scenario illustrated in Fig. 3.

A. Tests using simulated data

For simulation purpose, we make use of standard Monte Carlo simulations to estimate the root mean square error (RMSE) of the estimated target position over 10^2 independent trials. Moreover, the detection threshold is set to guarantee a nominal false failure detection probability of 10^{-2}. The parameters refer to three frequency modulated frequency modulated (FM) transmitters of opportunity, whereas receivers and target are set as in [15]. Specifically, the effective radiated power is 125 kW, the bandwidth is 50 kHz, the operating wavelength is 3 m, the receiver gain is -10 dBi, the noise figure is 25 dB, target radar cross section is 1 dBsm. To emulate a faulty sensor, all signals received at that specific receiver are enforced to have the noise component only.

In Fig. 4, the RMSE values evaluated for all points in the observed map are plotted to describe the accuracy reached by our algorithm for each possible target location in three different scenarios with 1, 2 and 3 sensors under failure, respectively. Precisely, considering a received signal of duration 1 ms, we focus on $V = 10$ sub-blocks

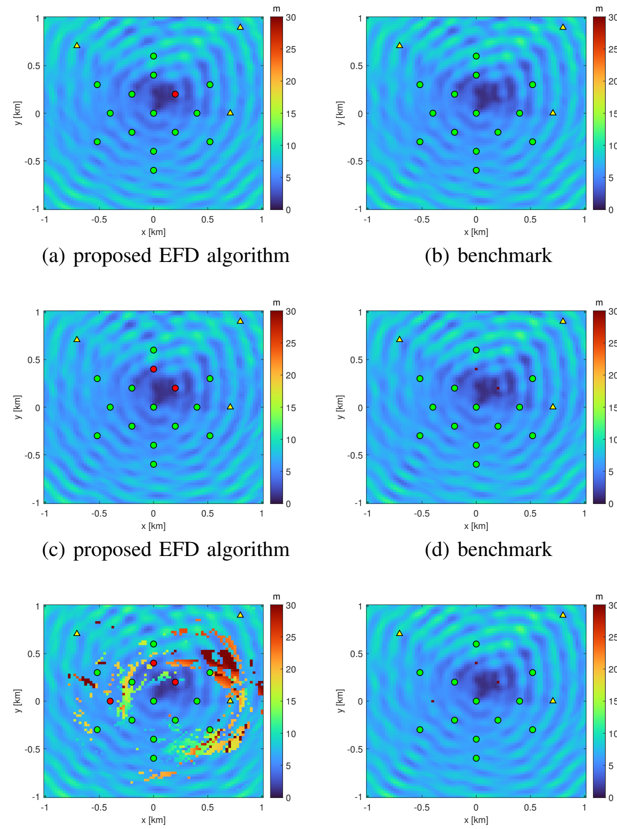

(a) proposed EFD algorithm (b) benchmark

(c) proposed EFD algorithm (d) benchmark

(e) proposed EFD algorithm (f) benchmark

Fig. 4. RMSE (m) of the target position for Fig. 3. Sensors (marked with the red circle) are in failure.

of 0.1 ms each, and for each of them the localization process is performed. Once the V position estimates are obtained, their median value is computed and used as the final estimate. By doing so, we ensure to reject final outliers in the measurements due to possible missed failures. The RMSE maps of the target position in Fig. 4 indicate that the proposed EFD almost reaches the same performance as its benchmark (i.e., the algorithm knowing the fault sensors) with 1 and 2 sensors under failure, while in the case of 3 anomalous sensors RMSE values of the target position are slightly higher than the considered benchmark.

To provide a quantitative measure of the achieved results, the following metric is evaluated

$$d_{\text{RMSE}}(\text{algorithm}, \text{benchmark}) = \frac{\|\mathbf{RMSE}_{\text{algorithm}} - \mathbf{RMSE}_{\text{benchmark}}\|_F}{\|\mathbf{RMSE}_{\text{benchmark}}\|_F}, \tag{2}$$

with $\|\cdot\|_F$ the Frobenius norm. Moreover, $\mathbf{RMSE}_{\text{algorithm}}$ and $\mathbf{RMSE}_{\text{benchmark}}$ denote the RMSE maps of the algorithm under consideration and the benchmark. The d_{RMSE} values are hence evaluated for the EFD and for its competitor not performing a failure detection, referred to as no failure detection (noFD). The respective results, reported in Table 1, show that the EFD error values exhibit shorter deviations from the benchmark performance than the noFD.

TABLE 1. d_{RMSE} values for the scenarios of Fig. 4.

	1 failure	2 failures	3 failures
d_{RMSE}(EFD, benchmark)	0.81	0.74	0.71
d_{RMSE}(noFD, benchmark,)	5.85	7.83	6.76

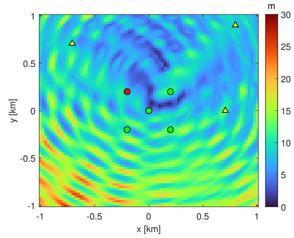

(a) proposed EFD algorithm

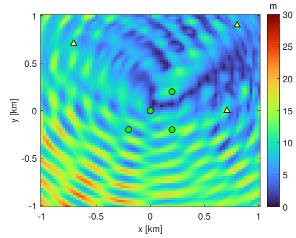

(b) benchmark

Fig. 5. RMSE (m) of the target position for Fig. 3 using real-recorded FM data. A sensor (marker with the red circle) is in failure.

B. Tests using real-recorded data

In this subsection, we test the EFD method in a partially simulated environment with the received signals acquired using a real system. More specifically, data are collected using the software defined radio (SDR) device "R820T2 RTL2832U RTL-SDR MCX" [16] and drawn from three different FM channels obtained setting the sample rate to 1.024 MHz. Hence, these data are used to emulate the signals from the transmitters of opportunity of Fig. 3(b), and the replicas for the receiving sensors are derived by adding white Gaussian noise in order to rule the specific value of SNR. To reduce the computational burden, 1000 samples are extracted from the acquired data that are in turn divided into $V = 4$ sub-blocks. Results in terms of RMSE are reported in Fig. 5 for the procedure repeated over 100 Monte Carlo trials.[2] As before, comparisons are performed using as benchmark the positioning algorithm a priori knowing the fault sensor. From the RMSE maps of the target position, it can be observed that the proposed method is capable of effectively rejecting the faulty sensor obtaining position estimation errors comparable to the benchmark. In fact, $d_{\text{RMSE}}(\text{EFD}, \text{benchmark}) = 1.15$, whereas $d_{\text{RMSE}}(\text{noFD}, \text{benchmark}) = 14.80$.

V. CONCLUDING REMARKS

A procedure to identify possible faulty sensors in a passive multistatic radar network has been proposed. Starting from the bistatic measurements, the method performs the detection of a faulty sensor exploiting the outlier distribution in the time delay measurements. The method groups the measurement equations into three clusters that quantify specific weights used to compute the warning scores of each sensor. Such scores are then used to declare whether or not each sensor is in failure. The sensors classified as faulty are removed from the set used to localize the target. Numerical results have shown the capability of the devised processing chain to correctly handle situations that includes anomalous sensors with localization errors close to the benchmark. In future works, it would be of interest the classification of the sensor failure by identifying the causes.

[2]In the simulation performed using real-recorded data, the same parameter setting as in the previous analyses is applied.

ACKNOWLEDGMENT

The work of Linjie Yan was supported by the National Natural Science Foundation of China under Grant 62201564.

REFERENCES

[1] R. Klemm, U. Nickel, C. H. Gierull, and P. Lombardo, *Novel Radar Techniques and Applications: Real Aperture Array Radar, Imaging Radar, and Passive and Multistatic Radar*. IET, 2017, vol. 1.

[2] H. Kuschel, D. Cristallini, and K. E. Olsen, “Tutorial: Passive Radar Tutorial,” *IEEE Aerospace and Electronic Systems Magazine*, vol. 34, no. 2, pp. 2–19, 2019.

[3] A. Asif and S. Kandeepan, “Cooperative Fusion Based Passive Multistatic Radar Detection,” *Sensors*, vol. 21, no. 9, p. 3209, 2021.

[4] M. Malanowski, “An Algorithm for 3D Target Localization from Passive Radar Measurements,” in *Photonics Applications in Astronomy, Communications, Industry, and High-Energy Physics Experiments 2009*, vol. 7502. SPIE, 2009, pp. 376–381.

[5] M. Malanowski and K. Kulpa, “Two Methods for Target Localization in Multistatic Passive Radar,” *IEEE Transactions on Aerospace and Electronic Systems*, vol. 48, no. 1, pp. 572–580, 2012.

[6] G. Battistelli, L. Chisci, S. Morrocchi, F. Papi, A. Farina, and A. Graziano, “Robust Multisensor Multitarget Tracker with Application to Passive Multistatic Radar Tracking,” *IEEE Transactions on Aerospace and Electronic Systems*, vol. 48, no. 4, pp. 3450–3472, 2012.

[7] P. Falcone, F. Colone, A. Macera, and P. Lombardo, “Two-Dimensional Location of Moving Targets within Local Areas using WiFi-Based Multistatic Passive Radar,” *IET Radar, Sonar & Navigation*, vol. 8, no. 2, pp. 123–131, 2014.

[8] A. J. Wileman and S. Perinpanayagam, “Failure Mechanisms of Radar and RF Systems,” *Procedia CIRP*, vol. 11, pp. 56–61, 2013.

[9] J. S. Picard and A. J. Weiss, “Bounds on the Number of Identifiable Outliers in Source Localization by Linear Programming,” *IEEE Transactions on Signal Processing*, vol. 58, no. 5, pp. 2884–2895, 2010.

[10] I. Enosh and A. J. Weiss, “Outlier Identification for TOA-based Source Localization in the Presence of Noise,” *Signal processing*, vol. 102, pp. 85–95, 2014.

[11] M. Compagnoni, A. Pini, A. Canclini, P. Bestagini, F. Antonacci, S. Tubaro, and A. Sarti, “A Geometrical–Statistical Approach to Outlier Removal for TDOA Measurements,” *IEEE Transactions on Signal Processing*, vol. 65, no. 15, pp. 3960–3975, 2017.

[12] G. Giunta, L. Pallotta, and D. Orlando, “Detecting Sensor Failures in TDOA-based Passive Radars: A Statistical Approach based on Outlier Distribution,” *IEEE Transactions on Aerospace and Electronic Systems*, vol. 59, no. 3, pp. 2176–2187, 2023.

[13] L. Pallotta and G. Giunta, “Accurate Delay Estimation for Multisensor Passive Locating Systems Exploiting the Cross-Correlation between Signals Cross-Correlations,” *IEEE Transactions on Aerospace and Electronic Systems*, vol. 58, no. 3, pp. 2568–2576, 2022.

[14] H. Fitriyah and A. S. Budi, “Outlier Detection in Object Counting based on Hue and Distance Transform using Median Absolute Deviation (MAD),” in *International Conference on Sustainable Information Engineering and Technology (SIET)*. IEEE, 2019, pp. 217–222.

[15] J. W. Brown, “FM Airborne Passive Radar,” Ph.D. dissertation, UCL (University College London), 2013.

[16] R. W. Stewart, K. W. Barlee, D. S. W. Atkinson, and L. H. Crockett, *Software Defined Radio using MATLAB & Simulink and the RTL-SDR*. Strathclyde Academic Media, 2015.